JCI insight

Low-dose interleukin-2 shapes a tolerogenic gut microbiota that improves autoimmunity and gut inflammation

Nicolas Tchitchek, … , Harry Sokol, David Klatzmann

JCI Insight. 2022. https://doi.org/10.1172/jci.insight.159406.

Research In-Press Preview **Therapeutics**

Gut microbiota (GM) dysbiosis is associated with inflammatory bowel diseases and also with cardiometabolic, neurologic, and autoimmune diseases. GM composition has a direct effect on the immune system, and vice versa, and particularly on regulatory T cell (Treg) homeostasis. Low-dose interleukin-2 (IL-2_{LD}) stimulates Tregs and is a promising treatment for autoimmune and inflammatory diseases. We aimed to evaluate the impacts of IL-2_{LD} on GM, and correlatively on the immune system. We used 16S ribosomal RNA profiling and metagenomics to characterize GM of mice and humans treated or not with IL-2_{LD}. We performed faecal microbiota transplantation (FMT) from IL-2_{LD}-treated to naïve recipient mice and evaluated its effects in models of gut inflammation and diabetes. IL-2_{LD} markedly affects GM composition in mice and humans. Transfer of an IL-2-tuned microbiota by FMT protected C57BL/6J mice from dextran sulphate sodium-induced colitis and prevented diabetes in NOD mice. Metagenomic analyses highlighted a role for several species impacted by IL-2_{LD} and for microbial pathways involved in the biosynthesis of amino acids, short-chain fatty acids, and L-arginine. Our results demonstrate that IL-2_{LD} induces changes in GM that are involved in the immunoregulatory effects of IL-2_{LD} and suggest a cross-talk between Tregs and GM. These results provide novel insights for understanding the mode of action of Treg-directed therapies.

Low-dose interleukin-2 shapes a tolerogenic gut microbiota that improves autoimmunity and gut inflammation.

Nicolas Tchitchek[1], Otriv Nguekap Tchoumba[1,2†], Gabriel Pires[1†], Sarah Dandou[1], Julien Campagne[1], Guillaume Churlaud[1,2], Gwladys Fourcade[1], Thomas W. Hoffmann[3], Francesco Strozzi[4], Camille Gaal[4], Christophe Bonny[4], Emmanuelle Le Chatelier[5], Dusko Erlich[5], Harry Sokol[3,6,7] and David Klatzmann[1,2*]

[1]Sorbonne Université, INSERM, Immunology-Immunopathology-Immunotherapy (i3), F-75005 Paris, France.

[2]AP-HP, Hôpital Pitié-Salpêtrière, Biotherapy (CIC-BTi) and Inflammation-Immunopathology-Biotherapy Department (i2B), F-75013, Paris, France.

[3]Micalis Institute, Institut National de la Recherche Agronomique (INRA), AgroParisTech, Univ Paris-Saclay ; F-78352, Jouy-en-Josas, France.
Sorbonne University-UPMC Univ Paris 06, INSERM ERL 1157, Avenir Team Gut Microbiota and Immunity, UMR 7203; F-75005, Paris, France.

[4]Enterome, 94/96 Avenue Ledru-Rollin, 75011 Paris, France

[5]MetaGenoPolis, INRA, Université Paris-Saclay, 78350, Jouy-en-Josas, France.

[6]Sorbonne Université, Ecole Normale Supérieure, CNRS, INSERM, AP-HP, Laboratoires des Biomolécules (LBM) ; F-75012, Paris, France.

[7]AP-HP, Hôpital Saint Antoine, Department of Gastroenterology and Inflammation-Immunopathology-Biotherapy Department (i2B), F-75011, Paris, France.

† These authors contributed equally to this work

* To whom correspondence should be addressed: David Klatzmann, Clinical Investigation Center for Biotherapies (CIC-BTi), Pitié-Salpêtrière Hospital, 83 bd de l'hôpital, 75651 Paris, France. Email: david.klatzmann@sorbonne-universite.fr

Funding

Assistance Publique-Hôpitaux de Paris, Investissements d'Avenir programme (ANR-11-IDEX-0004-02, LabEx Transimmunom and ANR-16-RHUS-0001, RHU iMAP).

Conflict-of-interest statement

The authors have no conflict of interest to declare.

Keywords: tolerance, immunoregulation, immuno-metabolism, systems immunology, microbiome, faecal transplantation, inflammatory bowel diseases

ABSTRACT

Gut microbiota (GM) dysbiosis is associated with inflammatory bowel diseases and also with cardiometabolic, neurologic, and autoimmune diseases. GM composition has a direct effect on the immune system, and vice versa, and particularly on regulatory T cell (Treg) homeostasis. Low-dose interleukin-2 (IL-2_{LD}) stimulates Tregs and is a promising treatment for autoimmune and inflammatory diseases. We aimed to evaluate the impacts of IL-2_{LD} on GM, and correlatively on the immune system. We used 16S ribosomal RNA profiling and metagenomics to characterize GM of mice and humans treated or not with IL-2_{LD}. We performed faecal microbiota transplantation (FMT) from IL-2_{LD}-treated to naïve recipient mice and evaluated its effects in models of gut inflammation and diabetes. IL-2_{LD} markedly affects GM composition in mice and humans. Transfer of an IL-2-tuned microbiota by FMT protected C57BL/6J mice from dextran sulphate sodium-induced colitis and prevented diabetes in NOD mice. Metagenomic analyses highlighted a role for several species impacted by IL-2_{LD} and for microbial pathways involved in the biosynthesis of amino acids, short-chain fatty acids, and L-arginine. Our results demonstrate that IL-2_{LD} induces changes in GM that are involved in the immunoregulatory effects of IL-2_{LD} and suggest a cross-talk between Tregs and GM. These results provide novel insights for understanding the mode of action of Treg-directed therapies.

INTRODUCTION

Autoimmune diseases intrinsically reveal dysregulation of the balance between regulatory and effector immune responses, hence Treg insufficiency (1, 2). Low-dose interleukin-2 (IL-2_{LD}) expands and activates Tregs, and thus has a very broad potential for the treatment of numerous autoimmune, inflammatory or allergic diseases (2). Furthermore, IL-2_{LD} has pleiotropic effects that can be beneficial in autoimmune diseases, notably the inhibition of the differentiation of naive CD4 cells into pro-inflammatory T helper (Th) 17 and T follicular helper (Tfh) cells (3, 4). As the therapeutic potential of IL-2 is currently being investigated in many autoimmune diseases, understanding its mode of action is of prime importance for rational drug development.

Treg cells are usually defined in humans as $CD4^+Foxp3^+CD25^+CD127^{low}$ cells, although some Tregs may express a low level of CD25, and as $CD4^+Foxp3^+$ cells in mice. Their main role is to control self-tolerance and inflammation. Indeed, experimental ablation of Tregs immediately triggers severe inflammation, including of the gut, and the development of multiorgan autoimmune diseases (5). Tregs also have important roles in tissue regeneration (6), including in the intestine. IL-2 is the non-redundant key cytokine for the differentiation, survival, and function of Tregs. Mutations of the IL-2 signalling pathway in humans and mice are associated with systemic inflammation linked to Treg deficiencies (2). Tregs meet their metabolic requirements by utilizing fatty acids and pyruvate oxidation, in contrast to effector T cells, which mainly rely on glycolysis.

The composition of gut microbiota (GM) is linked to human health and diseases and is in a dynamic interplay with the immune system (7–10). GM composition has a direct effect on the immune environment and vice versa (9, 10). Many factors – including diet (11), environmental exposure (12), or antibiotics (13) – can modify microbiota composition, possibly leading to altered immune homeostasis (14, 15) and secondarily to disease induction. The effects of GM

on immune regulation are in part linked to Treg generation and proliferation in Peyer's patches (PP) and mesenteric lymph nodes (16, 17). Treg homeostasis in the intestine is mainly controlled by commensal microbial metabolism (18, 19). Tregs from PP and intestinal mucosa participate in the regulation of intestinal inflammation (20, 21). Thus, as IL2-$_{LD}$ expands and activates Tregs at a systemic but also tissue level, it has the potential to affect GM composition. Using 16S ribosomal RNA gene and metagenomic sequencing, we demonstrate that IL-2$_{LD}$ impacts GM composition in mice and humans. Moreover, we show that GM from IL-2$_{LD}$-treated animals can be efficiently transplanted to recipient mice that are then protected from gut inflammation and diabetes, demonstrating that the immunoregulatory effects of IL2$_{LD}$ are in part mediated by GM modulation.

RESULTS

IL-2_{LD} expands Tregs and protects from autoimmunity and gut inflammation

IL-2_{LD} has been shown to prevent and/or treat numerous autoimmune and inflammatory diseases (2). IL-2_{LD} is defined as a dosage that preferentially stimulates Tregs over effector T cells, which corresponds to doses of around 50,000 IU in mice and around 1 to 3 MIU in humans (2). We investigated the immunoregulatory effects of IL-2_{LD} in an inflammatory colitis model induced by the administration of DSS in drinking water of C57BL/6J mice. At the time of DSS administration, we treated the mice with IL-2_{LD} daily intraperitoneal injections for 5 days. Such treatment expands and activates Tregs systemically (2), including in the colon (22) and lamina propria (23). It led to significantly lower gut inflammation as evidenced by a much-reduced weight loss (**Figure 1A**) and disease activity index (**Figure 1B**) compared to controls.

We also investigated the effects of IL-2_{LD} on the prevention of spontaneous diabetes in non-obese diabetic (NOD) mice. In this model, diabetes occurs from around 20 to more than 50 weeks of age according to the experimental conditions, including animal housing. Thus, to obtain a long-term stimulation of Tregs without the need for potentially stressful daily injections, we administered IL-2 by means of a single injection of an IL-2-producing adeno-associated virus (AAV) vector (24) that allows long-term production of IL-2. The dose of vector administered was titrated such as to obtain a Treg activation and expansion similar to what is observed with daily intraperitoneal injections of IL-2_{LD}, and without a stimulation of effector T cells (24). Noteworthily, in the pancreas, this treatment expands Tregs without effects on Teffs, NK, and CD8+ cells (**Figure S1**). Thus, under the conditions used, the AAV-IL-2 treatment can be likened to an IL-2_{LD} treatment by daily injections in terms of Treg effects (**Figure 1C**). As a control for this procedure, we similarly administered a luciferase-producing AAV vector. Control NOD mice had a 60% rate of diabetes occurrence, while those treated with IL-2 were fully protected from diabetes (**Figures 1D**).

IL-2_{LD} impacts gut microbiota composition in mice

To determine if IL-2_{LD} supplementation induces changes in GM composition, we first performed 16S rRNA sequencing on feces from 4-week-old NOD and 6-week-old BALB/c mice treated with IL-2 by means of an AAV injection. As NOD mice have a genetically determined low expression of the *Il-2* gene (25), we hypothesized that this treatment could have a more pronounced effect on their gut microbiota compared to BALB/c mice.

The IL-2_{LD} treatment markedly modified GM composition in the faeces of NOD mice collected on day-30 after the AAV injection. These NOD mice were 8 weeks old at this timepoint, which is long before diabetes onset, which does not occur before 20 weeks in our NOD mouse colony. The abundances of 22 taxa were significantly modified in IL-2_{LD}-treated NOD mice compared to controls, 13 taxa being upregulated and 9 taxa being down-regulated (**Figure 2A**). The heatmap of the relative abundance of these 22 taxa, combined with unsupervised hierarchical clustering, highlighted that IL-2_{LD} induces modifications in the GM composition of NOD mice that allow a perfect separation of IL-2_{LD}-treated mice from untreated mice (**Figure 2A**).

As hypothesized, the GM composition was less impacted by the IL-2_{LD} treatment in BALB/c mice. Only 4 taxa were significantly modified in IL-2_{LD}-treated mice compared to controls (**Figure 2B**). In line with this observation, the heatmap of relative taxa abundances combined with unsupervised hierarchical clustering outlined that IL-2_{LD} induces GM modifications that did not allow a perfect separation of IL-2_{LD}-treated mice from untreated mice (**Figure 2B**).

These differences between the changes in microbiota induced by IL-2_{LD} in NOD and BALB/c mice prompted us to compare their GM composition before treatment. We observed remarkable differences for these mice raised in the same animal facility and fed with the same chow (**Figure 2C**). Heatmap of relative taxa abundances combined with unsupervised hierarchical clustering allowed a perfect separation of NOD and BALB/c mice (**Figure 2C**). Amongst the 22 taxa

dysregulated by IL-2_{LD} in NOD mice, *Intestinimonas* was enriched in BALB/c compared to NOD mice and was enriched by IL-2_{LD} in NOD mice. Reciprocally, *Parasutterella*, *Ruminococcaceae UCG−013*, and *ASF356* were less represented in BALB/c compared to NOD mice and were reduced by IL-2_{LD} in NOD mice (**Figure S2**).

Thus, IL-2_{LD} treatment, which confers protection against autoimmunity, is associated with GM changes in two distinct genetic backgrounds. Moreover, the GM of NOD mice, which have a genetically determined low IL-2 production (25), is the more impacted.

IL-2_{LD}-tuned gut microbiota can be transplanted and confers protection from autoimmunity and gut inflammation

As IL-2_{LD} modifies GM composition, which is in interplay with the immune system, we hypothesized that an IL-2_{LD}-tuned microbiota could participate in the immunoregulatory effects of IL-2_{LD}. We first verified that we could indeed transplant an IL-2_{LD}-tuned microbiota to naïve mice (so-called IL-2_{LD}-tuned FMT). NOD mice were treated with IL-2-producing or luciferase-producing AAV vectors, and their GM was collected 30 days thereafter. Collected microbiota were orally transferred in two groups of 6-week-old recipient NOD mice whose GM had been cleared with a cocktail of antibiotics (ATB) during the 14 days preceding FMT. 16S rRNA sequencing was performed on the recipient NOD mice after transplantation with IL-2_{LD}-tuned FMT or with control FMT. Multidimensional scaling representation of GM composition showed that the microbiota from IL-2-treated NOD donors could be efficiently transplanted, as it was similar to that of recipient mice (**Figure S3**). Furthermore, as shown in **Figure 3A,** 18 taxa were significantly different between recipients of GM from IL-2_{LD}-treated or control NOD mice (*i.e.* after FMT). Heatmap of relative taxa abundances combined with hierarchical clustering showed a perfect separation between NOD mice transplanted with an IL-2_{LD}-tuned or control GM. Six taxa were impacted by both IL-2_{LD} treatment and IL-2_{LD}-tuned FMT in

NOD mice (**Figure 3B**). Of these, *Desulfovibrio,* the *Lachnospiraceae bacterium A2* species, an uncultured genus of the *Ruminococcaceae* family, and an uncharacterized genus of the *Clostridiales vadinBB60 group* family were up- or down-regulated in a concordant manner in the two conditions.

As an IL-2_{LD}-tuned microbiota can be engrafted, we tested whether a transferred IL-2_{LD}-tuned microbiota could confer some protection against autoimmunity and gut inflammation. An IL-2_{LD}-tuned microbiota FMT did indeed significantly protect C57BL/6J mice from colitis induced by DSS. Weight loss (**Figure 3C**) and disease activity index (**Figure 3D**) were markedly and significantly reduced compared to untreated mice, to mice that received control FMT, and to mice treated with ATB. The mice having received ATB and no FMT behaved as the untreated control mice. This is not surprising as the colitis is induced two weeks after the ATB treatment, which leaves time for microbiota reconstitution.

Similarly, NOD mice that received IL-2_{LD}-tuned microbiota had a reduction of diabetes incidence compared to mice that received control FMT over the 50 weeks post-treatment (**Figure 3E**).

Altogether, these results show that an IL-2_{LD}-tuned microbiota can be efficiently transplanted to IL-2-naive recipient mice and protects against autoimmunity and gut inflammation in two murine genetic backgrounds. These results prompted us to analyze further the effects of IL-2 on GM by shotgun metagenomic sequencing.

Identification of microbiota species impacted by IL-2_{LD}

To further characterize the changes in GM composition induced by IL-2_{LD}, we performed gut microbiome profiling from IL-2_{LD}-treated NOD and C57BL/6J mice using shotgun metagenomics. The Simka algorithm was first used to quantify the effects of the IL-2 treatment between profiles without defining a prior metagenome reference (26).

Clustering based on the Jaccard distance perfectly separated NOD and C57BL/6J mice, and within these the IL-2_{LD}-treated from the untreated (**Figure 4A**), indicating that the NOD microbiota still differed from that of C57BL/6J mice after IL-2_{LD} treatment. We found that 13 taxa were dysregulated by IL-2_{LD} in C57BL/6J mice and 17 were dysregulated in NOD mice, with 8 species simultaneously impacted in the two mouse backgrounds (**Figure 4B**). *Akkermansia muciniphila* was upregulated by IL-2_{LD} in both mouse backgrounds. *Lactobacillus gasseri*, *Lactobacillus johnsonii*, *Lactobacillus reuteri* were down-regulated by IL-2_{LD} in both mouse backgrounds. Additionally, *Alistipes unclassified*, *Escherichia coli*, *Escherichia unclassified*, and *Parabacteroides goldsteinii* were dysregulated by IL-$2_{LD,}$ but with different directionalities.

Principal component analysis based on abundances clearly showed a strong effect of IL-2_{LD} in both genetic backgrounds (**Figure 4C** and **4D**). Noteworthily, these results were reproduced using an independent computational analysis (**Figures S4A** and **S4B**).

Identification of microbial functional pathways impacted by IL-2_{LD}

We next performed a functional analysis to gain more insight into microbial changes impacted by the IL-2_{LD} treatment. We found that IL-2_{LD} impacted 210 pathways in C57BL/6J mice and 92 pathways in NOD mice. Heatmaps of relative pathway abundances combined with hierarchical clustering showed a perfect separation between treated and untreated mice in both genetic backgrounds (**Figure 5A** and **5B**).

A total of 17 pathways were concordantly upregulated or down-regulated in both C57BL/6J and NOD mice relative to their respective untreated controls (**Figure 5C**). These pathways were mainly associated with biosynthesis, energy metabolism and glycan mechanisms – including L-arginine biosynthesis and inosine 5 phosphate biosynthesis – with many species contributing to these changes.

Overall, these results indicate that IL-2_{LD}-induced modifications in microbial populations profoundly impact pathways that could impact interaction with immune cells.

IL-2_{LD} treatment impacts the microbiome of patients with autoimmune diseases

We next assessed if IL-2_{LD} also influences GM in humans. We performed metagenomics profiling of feces samples from 6 patients with autoimmune diseases treated by IL-2_{LD} (TRANSREG trial, NCT01988506) (27). Feces were collected at baseline and between 3 to 6 months after treatment initiation.

We found 5 bacterial species impacted by IL-2_{LD} in patients (**Figure 6A**). At the functional level, we found 63 microbial pathways impacted by IL-2_{LD} in patients, all of them being down-regulated in samples obtained after IL-2_{LD} treatment relative to the respective baseline samples (**Figure 6B**). These pathways were mainly associated with nucleotide biosynthesis, biosynthesis, cofactor biosynthesis, amino acid biosynthesis, and degradation (**Figure 6C**). For each one of these pathways, we quantified the number of associated bacterial species (*i.e.*, the number of species expressing each given pathway). We found that the adenosine ribonucleotide de novo biosynthesis, super pathway of coenzyme A biosynthesis III, 5-aminoimidazole ribonucleotide biosynthesis I, UMP biosynthesis I, and methylerythritol phosphate pathways had the highest numbers of associated species (>80). L-arginine biosynthesis was also found to be impacted by IL-2_{LD} with multiple pathways having high numbers of associated species.

Noteworthily, the heatmaps of relative taxa abundances (**Figure 6A**) or of modified pathways (**Figure 6B**) combined with unsupervised hierarchical clustering, clustered well together the 6 pre-IL-2_{LD} GM and the 6 post-IL-2_{LD} GM of these patients.

DISCUSSION

We demonstrate here that IL-2 shapes GM, at both the taxonomic and functional levels, in three different murine genetic backgrounds and in patients with autoimmune diseases. Moreover, we show that IL-2-tuned microbiota can be transplanted and protects IL-2-naive recipient mice against experimental inflammatory bowel disease and diabetes.

IL-2_{LD} shapes fecal microbiota in different species

GM has the potential to shape the immune system (19, 28). In return, the immune system can have an impact on GM. Recently, modulation of expression of interleukin 17 (IL-17), a pro-inflammatory cytokine that contributes to both autoimmunity and host immune defence, has been reported to induce modifications of GM (29) that led to protection against central nervous system autoimmunity. Mirroring these observations, we show that a cytokine that expands and activates Tregs also shapes GM composition in three mouse genetic backgrounds and in humans. In mice, PCA and hierarchical clustering perfectly separated the microbiota of IL-2-treated versus control mice in the three genetic backgrounds, using two independent taxonomic profiling methods. Interestingly, the number of microbial taxa that change after IL-2_{LD} is always higher in NOD mice than in BALB/c or in C57BL/6J mice. As NOD mice have genetically controlled low IL-2 production that leads to Treg deficiency (25), this emphasizes the importance of the GM/IL-2/Treg axis in health and disease. Our results extend the recent observation that IL-2 leads to modification of GM in NOD mice using 16S rRNA analysis (23). Here, we extend this work by showing for the first time that IL-2-tuned microbiota has an immunoregulatory effect and by analyzing IL-2-treated human patients. We observed a clear impact of IL-2_{LD} on the microbiome in humans, although this impact was less pronounced than that observed in mice, likely due to higher inter-individual variability. Nevertheless, as for mice, we could accurately cluster together the pre-IL-2_{LD} GM and post-IL-2_{LD} GM from these

patients. This is remarkable. Indeed, given that diet as well as disease conditions profoundly affect GM composition, it could have been expected that pre- and post-IL-2_{LD} treatment samples from a given patient would have clustered together. Thus, based on the differentially abundant taxa and pathways, the robustness of the GM changes induced by IL-2_{LD} in humans is more discriminating than the individual's GM composition.

IL-2 licenses the gut microbiota to act as an immunomodulatory drug

The bidirectional interdependency of the GM and the immune system has raised the possibility that GM could modulate/mediate the efficacy of immunotherapies, which has indeed been observed for cancer immunotherapies (30–32). We report for the first time the ability of an immunomodulatory treatment targeting Tregs to confer its immunoregulatory potential on GM. This is important as alternatives to IL-2-producing AAV or IL-2 intraperitoneal injections have now been developed to stimulate Tregs. Among them is the use of IL-2 complexes with enhanced specificity for Tregs (33) or the use of the superagonistic anti-CD28 antibody (34). The impact of these Treg stimulation methods on the gut microbiome has yet to be studied.

Note that IL-2-tuned FMT results in control of two independent disease conditions, like the IL-2_{LD} treatment itself. Thus, IL-2_{LD} not only changes the composition of intestinal microbial taxa, but also licenses microbiota to act as an immunomodulatory treatment. This opens the interesting possibility of manipulating the microbiota before its transplantation, so as to improve its efficacy.

Gut microbiota modifications induced by IL-2 are relevant for the immunomodulatory effect of IL-2_{LD}-tuned microbiota

Our GM profiling provides some insights into the potential mechanisms by which IL-2_{LD} may impact the host. First, the majority of taxa differentially expressed in IL-2_{LD}-treated NOD mice

belong to the *Ruminococcaceae* family. Members of this family have been reported to be decreased in many autoimmune or inflammatory diseases, notably in patients with type 1 diabetes or Crohn's disease (35, 36). Second, taxa of *Intestinimonas*, the most differentially abundant genus in IL-2_{LD}-treated-NOD mice compared to controls, have been reported to be decreased in type 1 diabetes patients (35). *Intestinimonas* are also known to be producers of short-chain fatty acids, which are known to promote immunomodulation by favouring Tregs and limiting Teffs (37–39). Third, *Akkermansia muciniphila* is increased by IL-2_{LD} treatment in both NOD and C57BL6/J mice, and is more differentially abundant in IL-2-treated NOD mice than in IL-2-treated B6 mice. This taxon (i) has been described as a protector against autoimmunity in NOD mice and against DSS-induced colitis, and (ii) can also promote Tregs in inflammatory bowel diseases in mice (40, 41). Furthermore, the abundance of *Akkermansia muciniphila* has been shown to be associated with Treg proliferation (42). Fourth, Rowan et al. found that *Desulfovibrio* was significantly increased in acute and chronic human ulcerative colitis (43). Here, we found that this species was increased in IL-2_{LD}-treated NOD mice compared to untreated NOD mice, as well as in NOD mice with IL-2_{LD}-tuned FMT compared to NOD mice with control FMT. Additionally, the *Desulfovibrio species* was found to be upregulated in untreated NOD mice relative to untreated BALB/c mice.

Together, these observations point to a cross-talk between Tregs and these taxa that could provide at least part of the mechanism driving the immunoregulatory efficacy of FMT of IL-2-tuned microbiota.

Downstream of the modifications of taxa composition by IL-2_{LD}, we also identified functional pathways that could participate in the immunoregulatory efficacy of IL-2-tuned microbiota. We identified a core of 17 microbial metabolic pathways that change in both NOD and C57BL/6J mice after this IL-2_{LD} treatment. The biosynthesis of L-arginine, an amino acid described as a fuel for the generation of citrullinated peptides that could trigger autoimmune responses,

notably in type 1 diabetes (44–46), is decreased in intestinal microbes of IL2$_{LD}$-treated mice and humans. Conversely, metabolic pathways leading to the increase of short-chain fatty acids (*e.g.*, pyruvate fermentation to propanoate I) were increased by IL-2$_{LD}$ treatment in both murine genetic backgrounds. This observation is in line with our previous comment related to the major increase in *Intestinimonas,* known as short-chain fatty acid producers, in IL-2$_{LD}$-treated NOD mice. With the recent report that FMT from healthy donors halts the progression of new-onset type 1 diabetes in humans (47), our results suggest that the use of IL-2-tuned FMT or of FMT enriched in specific taxa could represent an improved treatment modality.

In summary, GM modifications induced by IL-2$_{LD}$ appear to favour taxa and microbe metabolic pathways that influence the Treg/Teff balance. Our results call for extended studies in human cohorts to confirm our observations. Our work suggests a virtuous circle in which IL-2$_{LD}$ impacts GM, and in return GM reinforces the primary effect of IL-2$_{LD}$ on Treg/Teff balance. It should be noted that Treg can shape GM (48), and it is also known that IL-2$_{LD}$ directly impacts Tregs. Thus, we can postulate that IL-2 may impact GM through the modulation of Tregs. This has implications for a better understanding of how GM participates in and maintains disease conditions and for the better design of immunoregulatory therapies, including improved FMT. The fact that IL-2-tuned microbiota act as an immunomodulatory treatment opens the possibility to manipulate GM for improved faecal microbiota transplantation and to discover microbial-derived molecules to treat autoimmune and inflammatory diseases. The effects of IL-2$_{LD}$-tuned FMT on the recipient immune system, notably at the level of the TCR repertoire of Tregs, have yet to be evaluated.

METHODS

Housing of mice and ethical statements

Female BALB/c mice, C57BL/6J mice, non-obese diabetic (NOD) mice, and NOD mice expressing GFP under the control Foxp3 gene promoter were maintained under pathogen-free conditions according to European legislation. All mice received the same food diet, which was normal-protein chow.

Administration of IL-2_{LD}

IL-2_{LD} was administered either: (i) by a single injection of an IL-2-producing recombinant adeno-associated virus vector serotype 8 (AAV8) (rAAV) vector, and compared to the injection of a luciferase-producing control rAAV, both at a concentration of 10^{10} rAAV viral genomes as previously described (24); or: (ii) by intraperitoneal injections with 50,000 units of ILT-101 (human recombinant interleukin 2; ILTOO Pharma) during five consecutive days, and compared to the injection of PBS.

Cytometry profiling

Cells were collected from NOD Foxp3 GFP mice. Blood were submitted to red blood cell lysis. Pancreas was digested with collagenase/DNase solution, and filtered, as previously described (49). Lamina propria cells were obtained with the Lamina Propria Dissociation Kit and the GentleMACS Octo Dissociator with Heaters (Miltenyi Biotec). For lamina propria, a Percoll density gradient step was performed as previously described (49). We used the following monoclonal antibodies at predetermined optimal dilutions for 20 min at 4 °C: Live-Dead-eFluor780, CD3-E450, CD8-SB600, CD4-HorizonV500, CD45-PE-CF594, and NKp46-Alexa700 (BD). Cells were acquired on a Cytoflex LX flow cytometer (Beckman Coulter) and

analyzed using FlowJo software (Tree Star, Inc.). Tregs were defined as GFP+ cells among CD4+ cells.

Monitoring of diabetes in NOD mice

Urinary glucose was measured every two days using colourimetric strips (Multistix, Bayer), and blood glucose was quantified by a glucometer (Optium Xceed, Abbott Diabetes Care). NOD mice were considered diabetic after 2 consecutive blood glucose readings above 250 mg/dL. In our hands, there is no reversal of diabetes after two such consecutive hyperglycemic readings (49), and mice have the classic accompanying histology of islet destruction. Note that the incidence of diabetes in NOD mice is known to vary depending on the cleanliness of the animal facilities.

Induction and monitoring of dextran sulphate sodium-induced colitis in C57BL/6J mice

Dextran sulphate sodium (DSS) was added to drinking water on day 0 (50). We used a concentration of 2% DSS in water. Mice were monitored three times a week for body weight, stool consistency, and the presence of blood in the stool (Disease Activity Index assessment).

Faecal Microbiota Transplantation

Before FMT, female mice were orally gavage-fed with 200 µL of a combination of metronidazole (1 g/L), vancomycin (500 mg/L), ampicillin (1 g/L), and neomycin sulphate (1 g/L) in sterile water for 14 days, as previously described (51, 52). Then, 200 mg of fresh stool (10 pellets) was suspended in 50 volumes of sterile water (1 mL) and 400 µL of this suspension was given to each recipient mouse by oral gavage using a 24G round tip gavage needle, for 2 consecutive days (53).

Mouse faecal DNA extraction and 16S rRNA gene sequencing

Mouse faecal genomic DNA was extracted and 16S rRNA sequenced as previously described (54).

Processing of 16S rRNA gene sequencing data

Raw read quality filtering was performed with the PRINSEQ-lite (55), using a Phred quality threshold of 30. Paired-end reads were assembled using FLASH with a minimum overlap of 30 bases, and a 97% overlap identity (56). Finally, CutAdapt was used to remove both forward and reverse primer sequences, with no mismatches allowed in those sequences (57).

Analysis of 16S rRNA sequencing data

Microbiota profiles were analyzed using QIIME2 based on the SILVA (release 132) database (58). Taxa with a cumulated abundance lower than 0.01% in the whole dataset were filtered out. Differentially abundant taxa were identified using a sparse partial least-squares discriminant analysis (sPLS-DA) approach with a feature selection based on an effect size for the Wilcoxon signed-rank test higher than 0.5.

Collection of human samples

Six patients from the TRANSREG trial (ClinicalTrials.gov; NCT01988506) (27) (two with Sjögren's disease, one with Crohn’s disease, one with Behçet’s disease, one with psoriasis, and one with systemic sclerosis) had available feces samples collected at baseline and between 3 to 6 months after the first IL-2_{LD} injection.

Human and mouse faecal metagenomic profiling

411 Total faecal DNA was shotgun sequenced using ion-proton technology (ThermoFisher),
412 resulting in 23.7±0.8 million (mean±SD) single-end short reads of 150 bases as a mean. Each
413 sample produced at least 20 million single-end DNA reads, from 45 to 370 bp.
414
415 **Processing of metagenomic sequencing data**
416 Raw reads were cleaned using AlienTrimmer to remove resilient sequencing adapters and low-
417 quality bases (59). Reads were filtered from human DNA and other possible food contaminant
418 DNA (using *Homo sapiens*, *Bos taurus*, and *Arabidopsis thaliana* assemblies and an identity
419 score threshold of 97%). Reads with a length <100 bp were removed.
420
421 **Analysis of metagenomic sequencing data**
422 MetaPhlAn2 and HUMAnN2 were used to assess the relative abundance of microbial
423 communities and microbial pathways (60, 61). Taxa with a cumulated abundance lower than
424 0.01% in the whole dataset were filtered out. Species and pathways differentially abundant
425 between conditions were identified using an sPLS-DA approach (62). Prior to the discriminant
426 analysis, a feature selection was performed to select species and pathways with an effect size
427 for a Wilcoxon signed-rank test higher than 0.5 for patients.
428
429 **Confirmatory principal component analysis of mouse metagenomic profiles**
430 The confirmatory principal component analysis was generated as described below. A gut
431 microbiome gene catalogue was built using bacterial genes extracted from proprietary Illumina
432 sequencing data of the gut microbiome from selected mouse strains (HDDR1, Taconix,
433 BALB/c and C57BL/6J) and the Illumina sequencing data from the public mouse microbiome
434 gene catalogue (63). This gut microbiome gene catalogue was built by performing metagenomic
435 assembly using MegaHit (v1.1.2) followed by gene prediction using GeneMark-HM (64), and

by clustering all the gene sequences at 95% identity over 90% length coverage, using CD-HIT (v4.7). All the sequencing data used for these steps were mapped back on the microbiome gene catalogue using BBmap, retaining only reads aligned with at least 95% identity and with a minimum length of 45 nucleotides. An abundance table was derived using the raw read counts of each gene. This abundance information was used by MSPminer to generate 761 MSPs (Metagenomic Species Pangenomes) (65).

High-quality sequencing data from the mouse strains analyzed in the present work were aligned against this newly constructed mouse gut microbiome gene catalogue using BBmap, with the same parameters as described above. Raw read gene counts were normalized by the gene length and scaled by the total number of reads per sample to generate relative abundance values for each gene. MSPs abundances were calculated by summing all the relative abundances of each gene belonging to a particular MSP and analyzed using R (v3.5) to perform the different statistical analyses. Principal component analysis was performed using the centred and scaled abundance values of the MSPs that were present in at least 70% of the samples (674 MSPs for NOD mice and 643 MSPs for C57BL/6 mice), using the prcomp function.

Statistics

The two-tailed Student's t-test was used to compare bodyweight variation, disease activity, and tregs abundance in treated and control mice at each timepoint. The χ^2 test was used to compare the Kaplan-Meier estimators. The Holm-Bonferroni adjustment was used for multiple-comparison correction. A P value less than 0.05 was considered significant.

Study approval

All procedures were approved by the Regional Ethics Committee on Animal Experimentation No. 5 of the Ile-de-France region (Ce5/2012/031).

Data and materials availability

16S rRNA gene sequencing and shotgun metagenomics sequencing data have been deposited in the SRA database and are available through the accession number PRJNA831236.

Author contributions

Concept, supervision and funding: DK. Mouse experiments: JC, GC, GF. 16S rRNA sequencing: TH, HS. Metagenomics shotgun sequencing: ELC, DE. Data analysis: all. Writing: NT, ONT, GP, SD, DK. All the authors revised the manuscript and approved its final version.

Acknowledgments

Funding was provided by the French National Research Agency (ANR-11-IDEX-0004-02, LabEx Transimmunom and ANR-16-RHUS-0001, RHU IMAP). Otriv Nguekap Tchoumba received a grant from SNFMI (Société Nationale Française de Médecine Interne).

REFERENCES

1. Sakaguchi S, et al. Foxp3+ CD25+ CD4+ natural regulatory T cells in dominant self-tolerance and autoimmune disease. *Immunol. Rev.* 2006;212:8–27.

2. Klatzmann D, Abbas AK. The promise of low-dose interleukin-2 therapy for autoimmune and inflammatory diseases. *Nat. Rev. Immunol.* 2015;15(5):283–294.

3. Liao W, Lin J-X, Leonard WJ. Interleukin-2 at the Crossroads of Effector Responses, Tolerance, and Immunotherapy. *Immunity* 2013;38(1):13–25.

4. Ritvo P-GG, et al. Tfr cells lack IL-2Rα but express decoy IL-1R2 and IL-1Ra and suppress the IL-1-dependent activation of Tfh cells. *Sci. Immunol.* 2017;2(15). doi:10.1126/sciimmunol.aan0368

5. Sakaguchi S, et al. Regulatory T cells and immune tolerance. *Cell* 2008;133(5):775–787.

6. Burzyn D, et al. A special population of regulatory T cells potentiates muscle repair. *Cell* 2013;155(6):1282–1295.

7. Tremaroli V, Bäckhed F. Functional interactions between the gut microbiota and host metabolism. *Nature* 2012;489(7415):242–249.

8. Clemente JC, Manasson J, Scher JU. The role of the gut microbiome in systemic inflammatory disease. *BMJ* 2018;360:j5145.

9. Erdman SE, et al. CD4+ CD25+ regulatory T lymphocytes inhibit microbially induced colon cancer in Rag2-deficient mice. *Am. J. Pathol.* 2003;162(2):691–702.

10. Ishikawa H, et al. Effect of intestinal microbiota on the induction of regulatory CD25+ CD4+ T cells. *Clin. Exp. Immunol.* 2008;153(1):127–135.

11. Maslowski KM, Mackay CR. Diet, gut microbiota and immune responses. *Nat. Immunol.* 2011;12(1):5–9.

12. Vatanen T, et al. Variation in Microbiome LPS Immunogenicity Contributes to Autoimmunity in Humans. *Cell* 2016;165(6):1551.

13. Yassour M, et al. Natural history of the infant gut microbiome and impact of antibiotic treatment on bacterial strain diversity and stability. *Sci. Transl. Med.* 2016;8(343):343ra81.

14. Kosiewicz MM, et al. Relationship between gut microbiota and development of T cell associated disease. *FEBS Lett.* 2014;588(22):4195–4206.

15. Willing BP, Russell SL, Finlay BB. Shifting the balance: antibiotic effects on host–microbiota mutualism. *Nat. Rev. Microbiol.* 2011;9(4):233–243.

16. Round JL, Mazmanian SK. Inducible Foxp3+ regulatory T-cell development by a commensal bacterium of the intestinal microbiota. *Proc. Natl. Acad. Sci. U. S. A.* 2010;107(27):12204–12209.

17. Cording S, et al. Commensal microbiota drive proliferation of conventional and Foxp3(+) regulatory CD4(+) T cells in mesenteric lymph nodes and Peyer's patches. *Eur. J. Microbiol. Immunol.* 2013;3(1):1–10.

18. Geuking MB, et al. Intestinal bacterial colonization induces mutualistic regulatory T cell responses. *Immunity* 2011;34(5):794–806.

19. Smith PM, et al. The microbial metabolites, short-chain fatty acids, regulate colonic Treg cell homeostasis. *Science* 2013;341(6145):569–573.

20. Panduro M, Benoist C, Mathis D. Tissue Tregs. *Annu. Rev. Immunol.* 2016;34:609–633.

21. Tanoue T, Atarashi K, Honda K. Development and maintenance of intestinal regulatory T cells. *Nat. Rev. Immunol.* 2016;16(5):295–309.

22. Goettel JA, et al. Low-Dose Interleukin-2 Ameliorates Colitis in a Preclinical Humanized Mouse Model. *Cell. Mol. Gastroenterol. Hepatol.* 2019;8(2):193–195.

23. Mullaney JA, et al. Type 1 diabetes susceptibility alleles are associated with distinct alterations in the gut microbiota. *Microbiome* 2018;6(1):35.

24. Churlaud G, et al. Sustained stimulation and expansion of Tregs by IL2 control autoimmunity without impairing immune responses to infection, vaccination and cancer. *Clin. Immunol. Orlando Fla* 2014;151(2):114–126.

25. Yamanouchi J, et al. Interleukin-2 gene variation impairs regulatory T cell function and causes autoimmunity. *Nat. Genet.* 2007;39(3):329–337.

26. Benoit G, et al. Multiple Comparative Metagenomics using Multiset k-mer Counting. *ArXiv160402412 Q-Bio* [published online ahead of print: September 23, 2016];http://arxiv.org/abs/1604.02412. cited July 1, 2021

27. Rosenzwajg M, et al. Immunological and clinical effects of low-dose interleukin-2 across 11 autoimmune diseases in a single, open clinical trial. *Ann. Rheum. Dis.* 2019;78(2):209–217.

28. Zegarra-Ruiz DF, et al. Thymic development of gut-microbiota-specific T cells. *Nature* 2021;594(7863):413–417.

29. Regen T, et al. IL-17 controls central nervous system autoimmunity through the intestinal microbiome. *Sci. Immunol.* 2021;6(56). doi:10.1126/sciimmunol.aaz6563

30. Iida N, et al. Commensal Bacteria Control Cancer Response to Therapy by Modulating the Tumor Microenvironment. *Science* 2013;342(6161):967–970.

31. Viaud S, et al. The Intestinal Microbiota Modulates the Anticancer Immune Effects of Cyclophosphamide. *Science* 2013;342(6161):971–976.

32. Gopalakrishnan V, et al. Gut microbiome modulates response to anti–PD-1 immunotherapy in melanoma patients. *Science* 2018;359(6371):97–103.

33. Boyman O, et al. Selective stimulation of T cell subsets with antibody-cytokine immune complexes. *Science* 2006;311(5769):1924–1927.

34. Lin C-H, Hünig T. Efficient expansion of regulatory T cells in vitro and in vivo with a CD28 superagonist. *Eur. J. Immunol.* 2003;33(3):626–638.

35. Qi C-J, et al. Imbalance of Fecal Microbiota at Newly Diagnosed Type 1 Diabetes in Chinese Children. *Chin. Med. J. (Engl.)* 2016;129(11):1298–1304.

36. Sokol H, et al. Faecalibacterium prausnitzii is an anti-inflammatory commensal bacterium identified by gut microbiota analysis of Crohn disease patients. *Proc. Natl. Acad. Sci. U. S. A.* 2008;105(43):16731–16736.

37. Furusawa Y, et al. Commensal microbe-derived butyrate induces the differentiation of colonic regulatory T cells. *Nature* 2013;504(7480):446–450.

38. Bui TPN, et al. Comparative genomics and physiology of the butyrate-producing bacterium Intestinimonas butyriciproducens. *Environ. Microbiol. Rep.* 2016;8(6):1024–1037.

39. Bui TPN, et al. Intestinimonas-like bacteria are important butyrate producers that utilize Nε-fructosyllysine and lysine in formula-fed infants and adults. *J. Funct. Foods* 2020;70:103974.

40. Bian X, et al. Administration of Akkermansia muciniphila Ameliorates Dextran Sulfate Sodium-Induced Ulcerative Colitis in Mice. *Front. Microbiol.* 2019;10:2259.

41. Hänninen A, et al. Akkermansia muciniphila induces gut microbiota remodelling and controls islet autoimmunity in NOD mice. *Gut* 2018;67(8):1445–1453.

42. Ansaldo E, et al. Akkermansia muciniphila induces intestinal adaptive immune responses during homeostasis. *Science* 2019;364(6446):1179–1184.

43. Rowan F, et al. Desulfovibrio bacterial species are increased in ulcerative colitis. *Dis. Colon Rectum* 2010;53(11):1530–1536.

44. Sodré FMC, et al. Peptidylarginine Deiminase Inhibition Prevents Diabetes Development in NOD Mice. *Diabetes* 2021;70(2):516–528.

45. Rondas D, et al. Citrullinated Glucose-Regulated Protein 78 Is an Autoantigen in Type 1 Diabetes. *Diabetes* 2015;64(2):573–586.

46. Buitinga M, et al. Inflammation-Induced Citrullinated Glucose-Regulated Protein 78 Elicits Immune Responses in Human Type 1 Diabetes. *Diabetes* 2018;67(11):2337–2348.

47. de Groot P, et al. Faecal microbiota transplantation halts progression of human new-onset type 1 diabetes in a randomised controlled trial. *Gut* 2021;70(1):92–105.

48. Wang S, et al. MyD88 Adaptor-Dependent Microbial Sensing by Regulatory T Cells Promotes Mucosal Tolerance and Enforces Commensalism. *Immunity* 2015;43(2):289–303.

49. Grinberg-Bleyer Y, et al. IL-2 reverses established type 1 diabetes in NOD mice by a local effect on pancreatic regulatory T cells. *J. Exp. Med.* 2010;207(9):1871–1878.

50. Chassaing B, et al. Dextran Sulfate Sodium (DSS)-Induced Colitis in Mice. *Curr. Protoc. Immunol. Ed. John E Coligan Al* 2014;104:Unit-15.25.

51. Ghosh S, et al. Colonic microbiota alters host susceptibility to infectious colitis by modulating inflammation, redox status, and ion transporter gene expression. *Am. J. Physiol. - Gastrointest. Liver Physiol.* 2011;301(1):G39–G49.

52. Brown K, et al. Prolonged antibiotic treatment induces a diabetogenic intestinal microbiome that accelerates diabetes in NOD mice. *ISME J.* 2016;10(2):321–332.

53. Markle JGM, et al. Sex differences in the gut microbiome drive hormone-dependent regulation of autoimmunity. *Science* 2013;339(6123):1084–1088.

54. Lamas B, et al. CARD9 impacts colitis by altering gut microbiota metabolism of tryptophan into aryl hydrocarbon receptor ligands. *Nat. Med.* 2016;22(6):598–605.

55. Schmieder R, Edwards R. Quality control and preprocessing of metagenomic datasets. *Bioinformatics* 2011;27(6):863–864.

56. Magoc T, Salzberg SL. FLASH: fast length adjustment of short reads to improve genome assemblies. *Bioinformatics* 2011;27(21):2957–2963.

57. Martin M. Cutadapt removes adapter sequences from high-throughput sequencing reads. *EMBnet.journal* 2011;17(1):10–12.

58. Bolyen E, et al. Reproducible, interactive, scalable and extensible microbiome data science using QIIME 2. *Nat. Biotechnol.* 2019;37(8):852–857.

59. Criscuolo A, Brisse S. AlienTrimmer: A tool to quickly and accurately trim off multiple short contaminant sequences from high-throughput sequencing reads. *Genomics* 2013;102(5–6):500–506.

60. Truong DT, et al. MetaPhlAn2 for enhanced metagenomic taxonomic profiling. *Nat. Methods* 2015;12(10):902–903.

61. Franzosa EA, et al. Species-level functional profiling of metagenomes and metatranscriptomes. *Nat. Methods* 2018;15(11):962–968.

62. Lê Cao K-A, Boitard S, Besse P. Sparse PLS discriminant analysis: biologically relevant feature selection and graphical displays for multiclass problems. *BMC Bioinformatics* 2011;12(1):253.

63. Lesker TR, et al. An Integrated Metagenome Catalog Reveals New Insights into the Murine Gut Microbiome. *Cell Rep.* 2020;30(9):2909-2922.e6.

64. Lomsadze A, et al. GeneMark-HM: improving gene prediction in DNA sequences of human microbiome. *NAR Genomics Bioinforma.* 2021;3(2). doi:10.1093/nargab/lqab047

65. Plaza Oñate F, et al. MSPminer: abundance-based reconstitution of microbial pan-genomes from shotgun metagenomic data. *Bioinformatics* 2019;35(9):1544–1552.

Figure legends

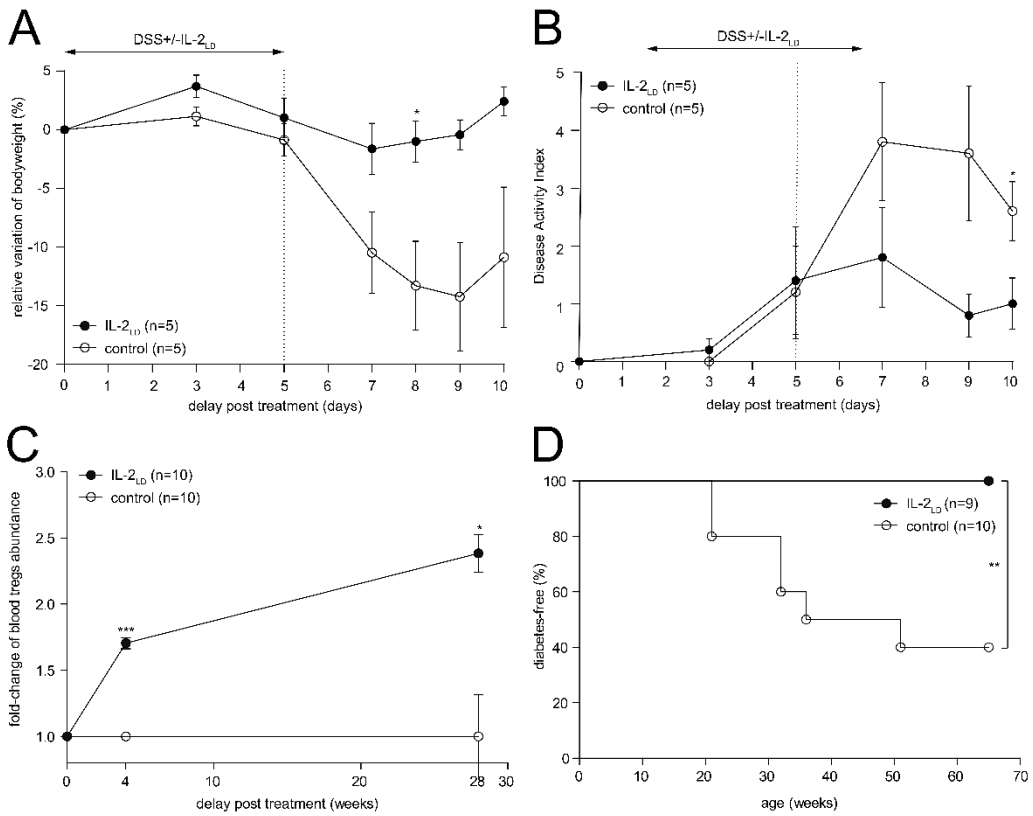

Figure 1 – IL-2$_{LD}$ protects from autoimmunity. (**A, B**) C57BL/6J female mice were treated or not with IL-2$_{LD}$ by means of intraperitoneal injections of IL-2 during 5 consecutive days. Dextran sulphate sodium (DSS) was administered in drinking water during the same 5 days. The body weight measurements expressed as percentages relative to baseline (**A**) and the Colitis Disease Activity Index (**B**) were evaluated at baseline and thereafter. (**C, D**) NOD female mice were treated or not with IL-2$_{LD}$ by means of IL-2-producing or luciferase-producing AAV vectors. (**C**) Fold changes of blood Tregs at baseline and after treatment. (**D**) Kaplan-Meier estimators of diabetes onset in NOD mice. Student's t-test was used to compare measurements in treated and untreated mice at each timepoint. The χ^2 test was used to compare the Kaplan-Meier estimators. The Holm-Bonferroni adjustment was used for multiple-comparison correction. Statistical significances are denoted as follows: * p-value < 0.05; ** p-value < 0.01;

*** p-value < 0.001. For each biological condition, the total number of mice used is provided in parentheses.

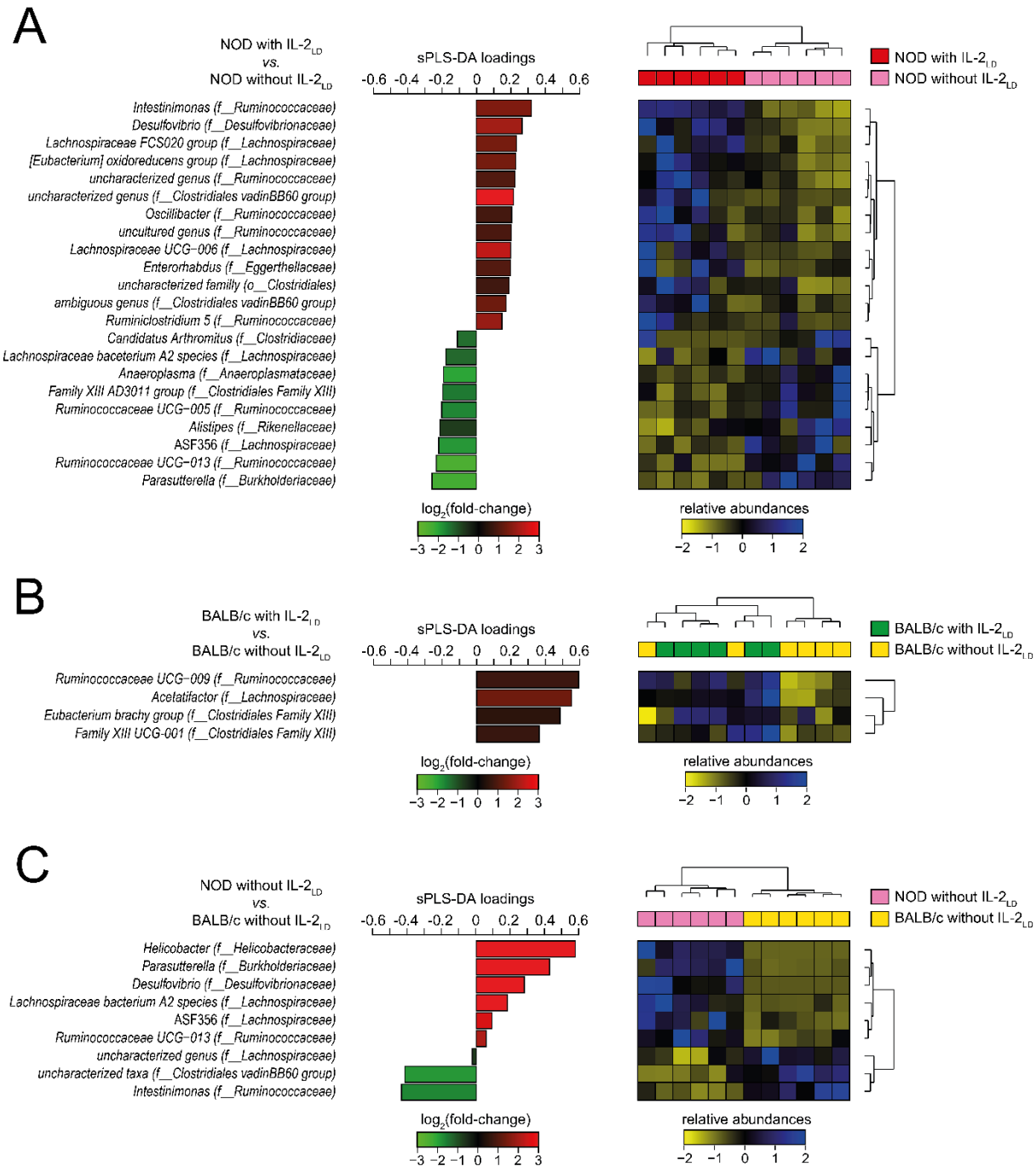

Figure 2 – IL-2$_{LD}$ impacts gut microbiota composition in mice. NOD and BALB/c mice were treated or not with IL-2$_{LD}$ by means of IL-2-producing or luciferase-producing AAV vectors. Profiling of their gut microbiota, collected 30 days after treatment, was performed using 16S rRNA sequencing. (**A** and **B**) Comparisons were made between NOD mice and

BALB/c mice treated or not with IL-2_{LD}. (**C**) An additional comparison was made between NOD mice and BALB/c mice without IL-2_{LD} to comprehend the gut microbial specificities associated with these mouse backgrounds. For each comparison, an sPLS-DA analysis was conducted to identify the gut microbial taxa best able to discriminate the conditions. The contribution of each taxon identified by the sPLS-DA analysis was represented using a horizontal bar of length proportional to its sPLS-DA loading. Horizontal bars were gradient-coloured based on the log2 of the taxa abundance fold-changes relative to the reference group. For each analysis, a heatmap of relative abundances combined with unsupervised hierarchical clustering was used to evaluate the capacity of the list of taxa to discriminate the conditions. The family (f__) or order (o__) associated with the taxa identified by the sPLS-DA analysis is indicated in parentheses.

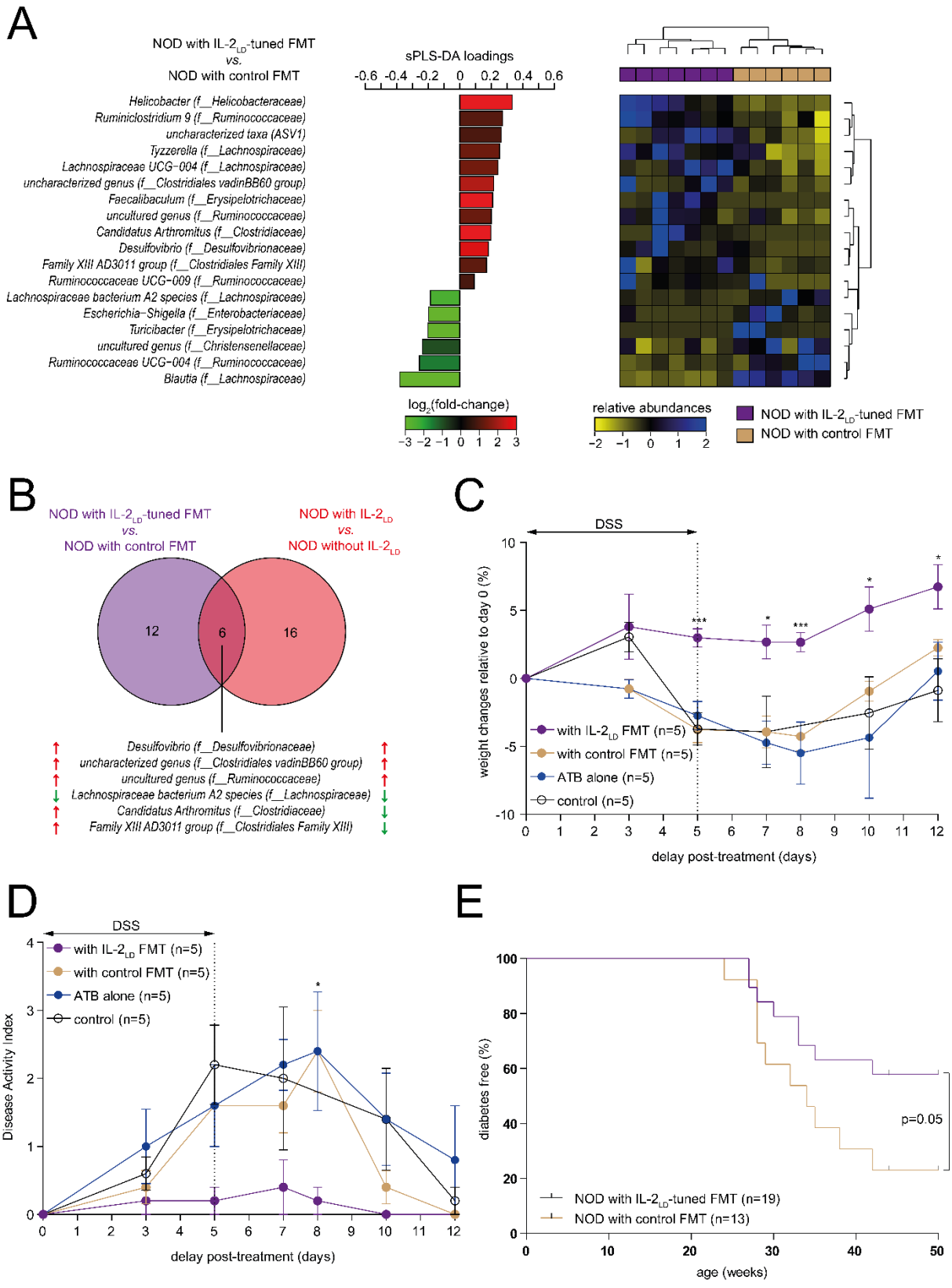

643

644 **Figure 3 – IL-2$_{LD}$-tuned gut microbiota protects from autoimmunity.** The microbiota of

645 IL-2$_{LD}$-treated NOD mice was transferred to recipient NOD mice treated by antibiotics (ATB)

646 during 14 days before faecal microbiota transplantation (FMT). NOD mice receiving FMT from

untreated NOD mice were used as controls. 16S rRNA sequencing was used to profile gut microbiota at day 30 post-treatment. (**A**) An sPLS-DA analysis was conducted to identify taxa separating NOD mice with FMT IL-2_{LD} from NOD mice with control FMT. The contribution of each taxon identified by the sPLS-DA analysis was represented using a horizontal bar of length proportional to its sPLS-DA loading. A heatmap of relative abundances combined with unsupervised hierarchical clustering was used to evaluate the capacity of the list of taxa to discriminate the conditions. (**B**) Venn diagram showing the overlap between the lists of taxa impacted by IL-2_{LD} and IL-2_{LD} FMT treatments relative to their control groups. (**C** and **D**) In an independent experiment, C57BL/6J mice were treated with IL-2_{LD}. Five weeks later, fresh stools from these mice were collected and orally administered to 7-week-old female C57BL/6 mice previously treated daily for 14 days with ATB. DSS was administered in drinking water during 5 days after transplantation to trigger colitis. Mouse body weight change (**C**) and Disease Activity Index (**D**) were evaluated until day 12. (**E**) In an independent experiment, 4-week-old female NOD mice were treated with IL-2_{LD} or without IL-2_{LD}. Five weeks later, fresh stools from these mice were collected and orally administered to 6-week-old female NOD mice previously treated daily for 14 days with ATB. Diabetes onset was screened for during the experiment. Student's t-test was used to compare measurements in treated and untreated mice at each timepoint. The Holm-Bonferroni adjustment was used for multiple-comparison correction. Statistical significances were reported as follows: * p-value < 0.05; ** p-value < 0.01; *** p-value < 0.001. IL-2_{LD} was administered or not to mice by means of IL-2-producing AAV. For each biological condition, the total number of mice used is provided in parentheses.

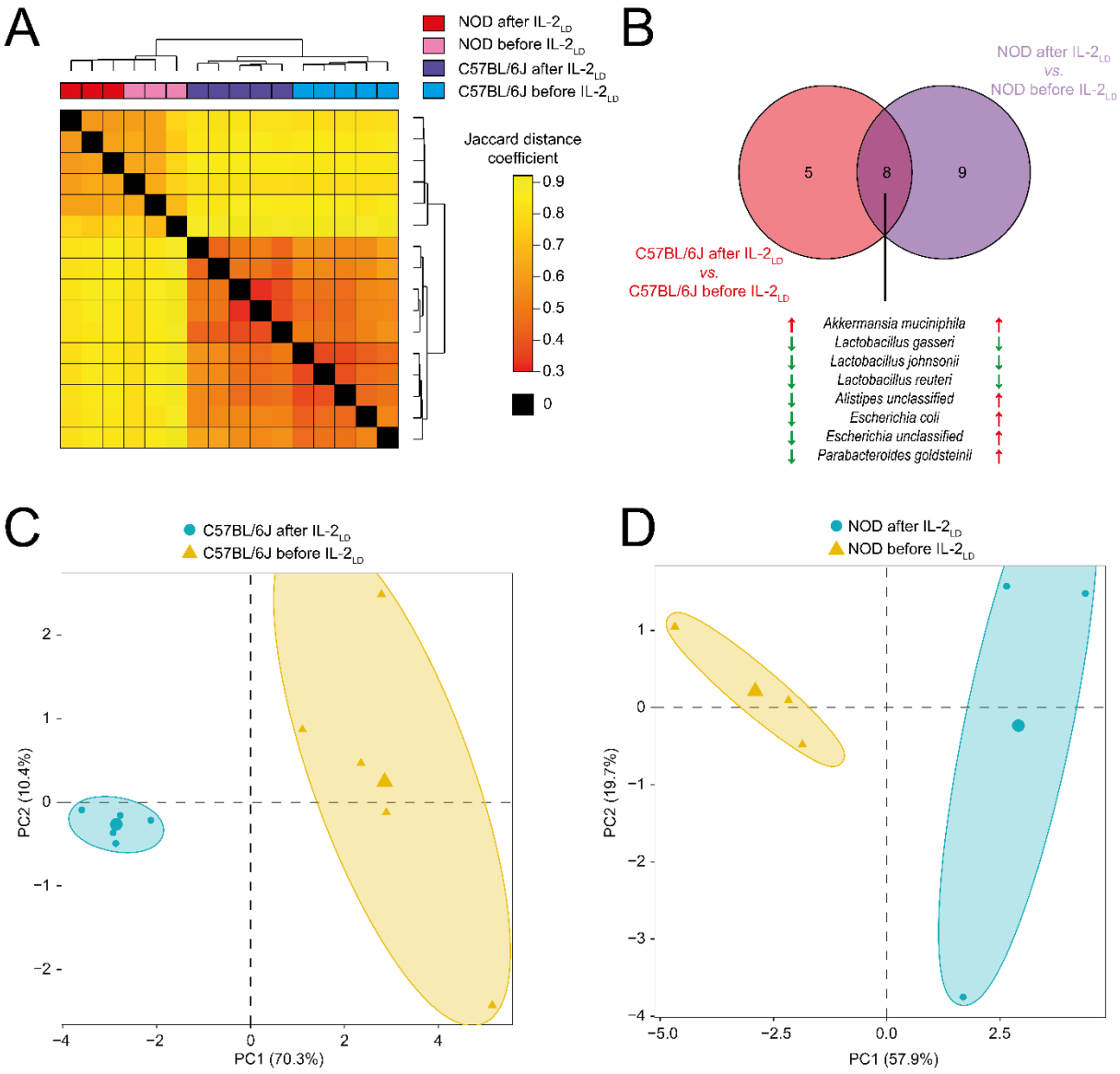

Figure 4 –Metagenomics reveals microbial species impacted by IL-2$_{LD}$. To gain more insight into the impact of IL-2$_{LD}$ on microbial composition, gut microbiome profiling of NOD and C57BL/6J mice before and 30 days after IL-2$_{LD}$ treatment was performed using metagenomics. (**A**) Distogram representation showing the distance between microbiome profiles. Similarities were calculated using the Simka algorithm, which compares profiles using a k-mer approach without needing a reference metagenome, and using the Jaccard distance coefficient on abundance levels. (**B**) Venn diagram showing the overlap between the lists of taxa significantly impacted by IL-2$_{LD}$ in NOD and C57BL/6J mice. The names of the overlapping species are indicated, and their upregulation and down-regulation relative to

679 controls are respectively indicated by red or green arrows. (**C** and **D**) Principal component
680 analysis representations of the gut microbiome profiles of NOD and C57BL/6J mice before and
681 after treatment with IL-2_{LD} generated using the abundance levels of taxa significantly impacted
682 by IL-2_{LD}. IL-2_{LD} was administered to mice by means of an IL-2-producing AAV vector.
683

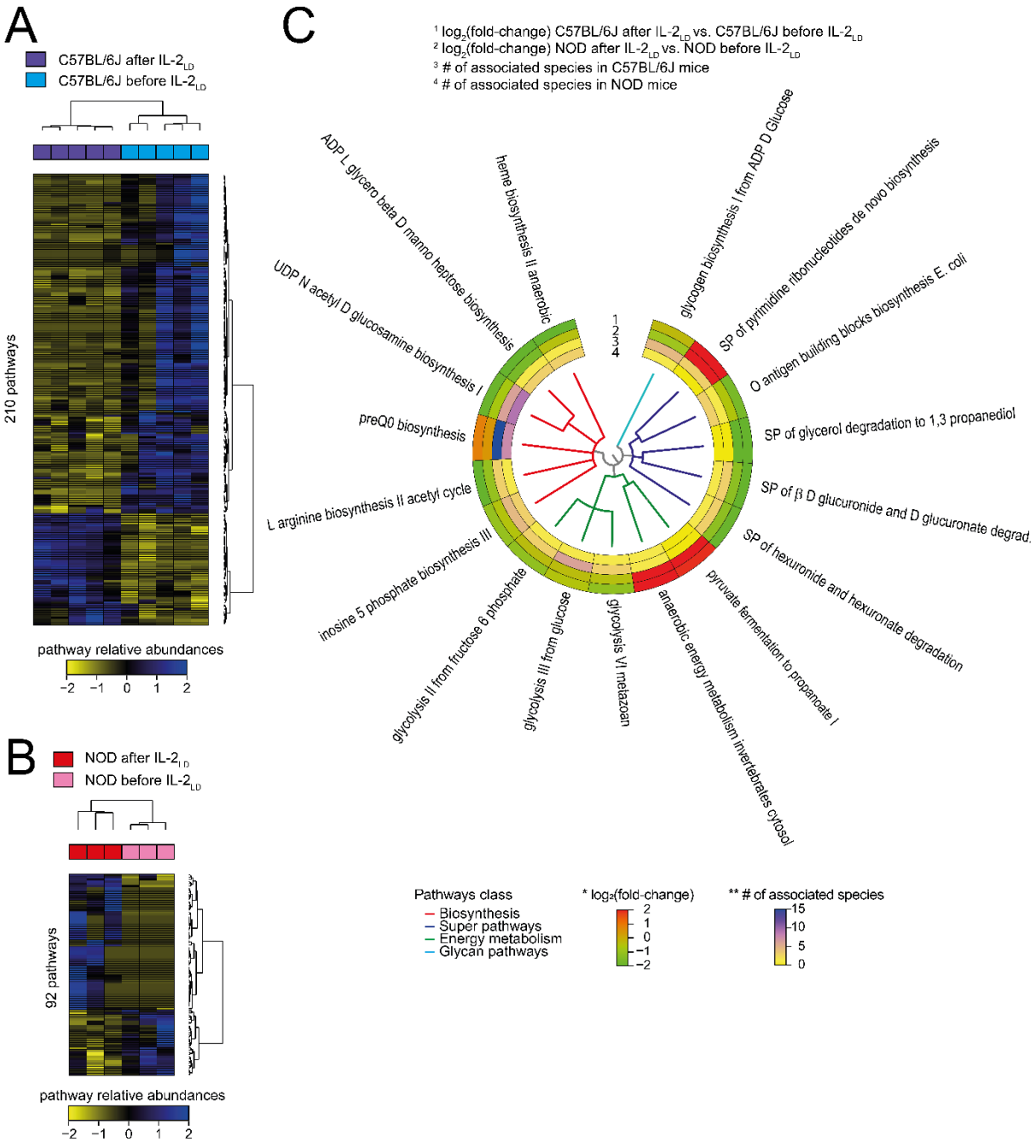

Figure 5 – Metagenomics reveals microbial pathways impacted by IL-2$_{LD}$. (**A** and **B**) Heatmap representations combined with unsupervised hierarchical clustering of relative abundance levels for microbial pathways impacted by the IL-2$_{LD}$ treatment in C57BL/6J and NOD mice relative to their baseline conditions. (**C**) Circular tree representation using colour-gradient scales showing the fold-change of microbial pathway abundances and the number of species associated for the 17 pathways impacted by IL2$_{LD}$ in both C57BL/6J and NOD mice

691 and with the same directionality. The classes of each pathway are also indicated in different
692 colours. IL-2_{LD} was administered to mice by means of an IL-2-producing AAV vector.
693

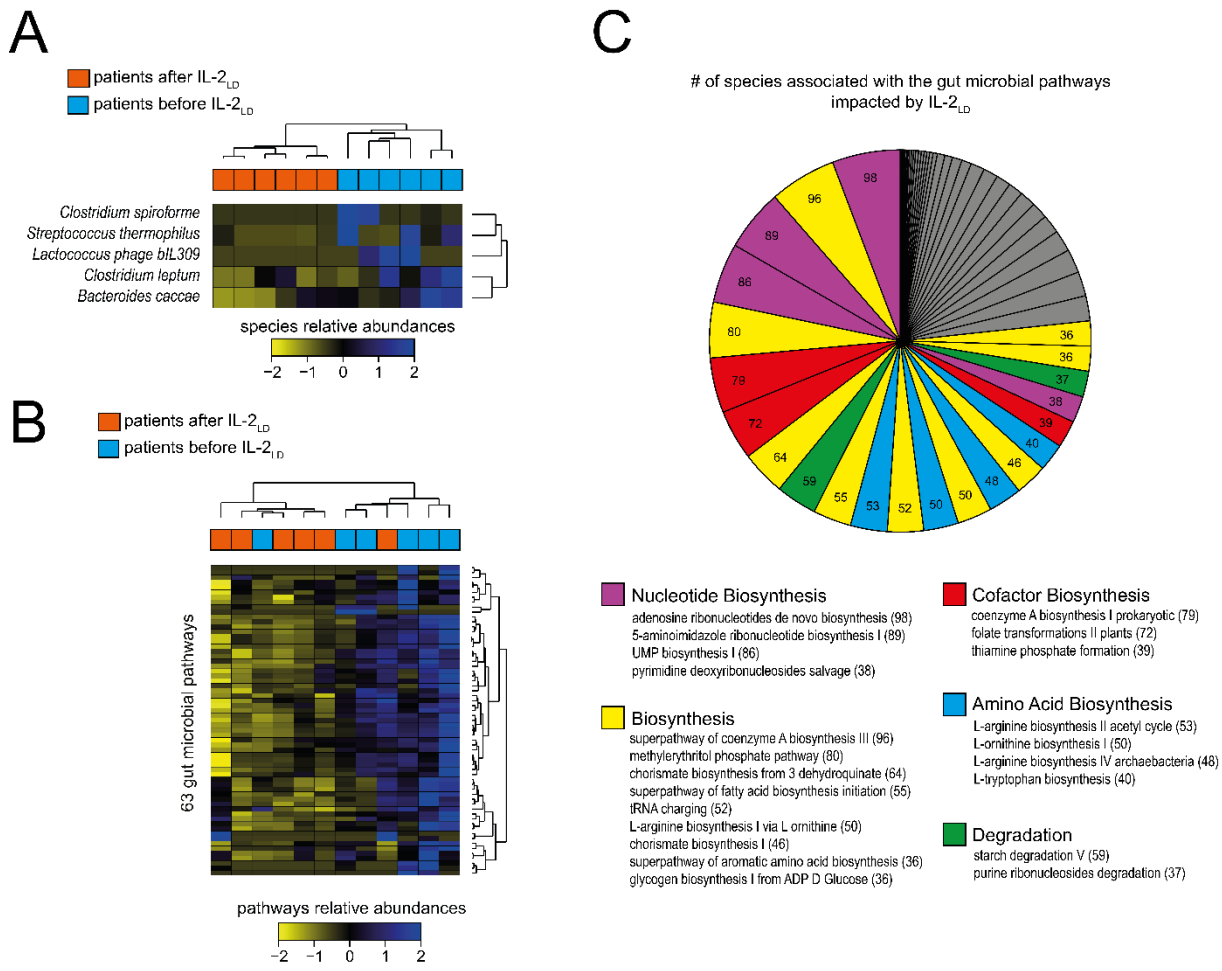

Figure 6 – IL-2$_{LD}$ impacts the gut microbiome in patients with autoimmune disorders. To evaluate the potential of IL2$_{LD}$ to modify the gut microbiome in humans, 6 patients with various autoimmune diseases were treated with IL-2$_{LD}$. Samples were collected at baseline and between 3 and 9 months after the first injection. Microbiome profiling was performed using metagenomics. (**A**) Heatmap representation of the relative abundances for the 5 bacterial species found to be differentially abundant in the gut microbiome of patients treated with IL-2$_{LD}$ relative to the baseline condition. (**B**) Heatmap representation of relative abundances for the 63 microbial pathways found to be differentially abundant in the gut microbiome of patients. (**C**) Circular pie chart showing the number of taxa associated with the microbial pathways differentially abundant in patients relative to baseline. Gut microbial pathways are coloured according to their classes. The number of contributing species is indicated in parentheses for each pathway. Pathways with fewer than 36 associated taxa are coloured in grey.